ABraytCSPfuture

Air-Brayton Cycle Concentrated Solar Power future plants via redox oxides-based structured thermochemical heat exchangers / thermal boosters

Deliverable D5.1

Optimized redox powders: scaled-up powder synthesis/processing protocols

Dissemination Level: PU

WP5 Manufacture of proof-of-concept-scale pressurized dual-bed unit from optimized materials compositions and porous structures

Date: 29.05.2025

https://www.abraytcspfuture.eu/

This project has received funding from the European Union's Horizon Europe research and innovation programme under grant agreement no 101084569.

Disclaimer

The work described in this document has been conducted within the ABraytCSPfuture project that is co-funded by the European Union. Views and opinions expressed herein are however those of the author(s) only and do not necessarily reflect those of the European Union or of the granting authority, European Climate, Infrastructure and Environment Executive Agency (CINEA). Neither the European Union nor the granting authority can be held responsible for them.

Grant Agreement Number: 101084569 Acronym: ABraytCSPfuture				
Full Title	**A**ir-**Brayt**on Cycle **C**oncentrated **S**olar **P**ower **future** plants via redox oxides-based structured thermochemical heat exchangers/thermal boosters			
Call Topic Identifier:	HORIZON-CL5-2021-D3-03			
Funding Scheme	HORIZON EUROPE, RIA – Research and Innovation Actions			
Project start date:	01.11.2022			
Project duration:	48 months			
Project URL	https://www.abraytcspfuture.eu/			
EU Project Officer	Clara Astudillo Llorente			
Project Coordinator	DLR – German Aerospace Center			
Deliverable	D5.1 – Optimized redox powders: scaled-up powder synthesis/processing protocols			
Date of Delivery	Contractual	30.04.2025	Actual	29.05.2025
Nature	Report			
Dissemination Level	Public			
Lead Beneficiary	CERTH			

Document History

Version	**Issue Date**	**Change History**	**Authors**	**Organisation**
1.0	28.04.2025	Document drafted	Chrysa Pagkoura, George Karagiannakis	CERTH
1.1	05.05.2025	Updated with final partner feedback	Christos Agrafiotis, David Vellas	DLR
1.2	12.05.2025	Updated with final partner feedback	Linfeng Yuan, Nicolaj Hornskov	LET
1.3	26.05.2025	Final Review	Dimitrina Lang	KB

About the Project

ABraytCSPfuture sets forth an innovative, carbon-neutral way for implementing the highly efficient air-Brayton gas turbine power generation cycles into future air-operated Concentrated Solar Power (CSP) plants. Air-Brayton cycles are used in traditional power plants where, however, involve fossil fuels combustion via pressurized air. *ABraytCSPfuture*'s carbon-neutral approach aims at achieving higher solar-to-electricity efficiencies, vital for competitiveness of CSP and non-reachable by either PVs or molten salts and thermal oils, increasing in parallel significantly the plants' storage capability. The project will develop and demonstrate a first-of-its-kind compact, dual-bed thermochemical reactor/heat exchanger unit that will transfer heat from a non-pressurised air stream to a pressurised one, while also operating as a thermal booster, raising the temperature of the pressurized stream to the level required for Brayton cycles. Furthermore, the volumetric solar energy storage density of air-operated CSP plants will be significantly increased by rendering their current sensible-only regenerative storage systems to hybrid sensible-thermochemical storage ones within the same storage volume. Both these functionalities will be materialized by thermochemical reactor/heat exchanger units comprised of non-moving, flow-through porous ceramic structures (honeycombs or foams) based on earth-abundant, cost-efficient, non-toxic oxide materials and exploiting reversible reduction/oxidation reactions of such oxides in direct contact with air, accompanied by significant endothermic/exothermic heat effects. The proposed technology is set forth by an interdisciplinary partnership spanning the entire CSP value chain, comprised of leading research centres, universities, innovative SMEs and large enterprises, including ancillary services providers and technology end-users.

Deutsches Zentrum fuer Luft- und Raumfahrt e.V., **DLR**	DE	DLR
Centre for Research & Technology Hellas, **CERTH**	EL	CERTH CENTRE FOR RESEARCH & TECHNOLOGY HELLAS
University of Twente, **UT**	NL	UNIVERSITY OF TWENTE.
Fundación CENER, **CENER**	ES	CENER NATIONAL RENEWABLE ENERGY CENTRE ADItech
Fundación TEKNIKER, **TEKN**	ES	Tekniker
Fraunhofer Gesellschaft zur Foerderung der angewandten Forschung e.V., **FHG (IWKS)**	DE	Fraunhofer IWKS
OPRA Turbines, **OPRA**	NL	Destinus
KRAFTBLOCK GmbH, **KB**	DE	KRAFT BLOCK
LANDSON Emission Technologies A/S, **LET**	DK	landson
COBRA Instalaciones y Servicios S.A., **COBRA**	ES	cobra

Table of Contents

This deliverable is part of a project that has received funding from the European Union's Horizon Europe research and innovation programme under grant agreement no 101084569

Executive Summary

The present deliverable relates to the protocols for scaled-up powder synthesis with the aim of achieving relatively optimum redox structures at a scale/quantity to cover the needs of the envisaged proof-of-concept pressurized dual-bed unit in the framework of the necessary experimental work of WP5. This deliverable is closely linked with deliverable D3.3 and provides the roadmap to a practical scaled-up manufacturing of redox structures for the needs of the project and beyond.

The qualified strategy is to **mix the raw powders** of the targeted composition, shape the **scaled-up structures from this mixture** and calcine the structured raw mixture, thereby achieving **synthesis of the perovskite and the necessary sintering of the body in a single step**. As already mentioned in D3.3, this has certain advantages and some challenges but its in-principle feasibility has already been validated in WP3. The targeted composition is primarily $Ca_{0.90}Sr_{0.10}MnO_3$ (CS10MO) but two additional compositions based on CS10MO with Fe-doping in the B-site (i.e. CS10MF5O and CS10MF10O) are also under consideration at the time of preparation of this document. Thus, the raw powders include $CaCO_3$, Mn_2O_3, $SrCO_3$ and Fe_2O_3. All of them are relatively abundant and low-cost materials.

In the last part of this document, the findings of the work carried out so far via following this protocol are reported and the general workplan on how to proceed to achieve the manufacture of proof-of-concept-scale dual-bed unit from porous structures and guide the relevant work of WP5 is provided.

Changes with respect to the DoA

There are no major changes or deviations with respect to the relevant provisions of the DoA in the project's GA. The deliverable has been submitted with approximately one month delay as compared to its initial scheduled date due to slight delays associated with the profound challenges of identifying the most favourable scaling-up protocol to achieve in-principle feasible manufacturing of scaled-up extruded honeycombs. This slightly delayed submission had no impact on other tasks.

1. Introduction

The document starts with a summary of qualified compositions so far and the comparative evaluation/characterization results obtained from structures manufactured from pre-synthesized powders versus the ones obtained from extrusion of raw mixtures and subsequent calcination. The next important part relates to results on the feasibility to prepare scaled-up structures by following the latter manufacturing strategy and the necessary applicable measures to achieve this. The term ''scaled-up structures'' addresses sizes like or comparable to the ones already outlined in deliverable D3.3 and which are relevant to the needs of the building blocks required to assemble the proof-of-concept unit of WP5. As explained in D3.3, the qualified shaping method is extrusion to achieve honeycomb-like redox monoliths. The plan to ensure that the necessary blocks are compatible and ready on time to build the WP5 proof-of-concept unit is presented at the end of this document.

2. Final qualified compositions for scaled-up structures & general plan for shaping

As already defined in deliverable D2.4 and subsequently updated/validated in deliverables D3.1, D3.2 and D3.3, the qualified redox powder compositions for the preparation of structures required by WP5 are **$Ca_{0.90}Sr_{0.10}MnO_3$/CS10MO** (primary choice) and $Ca_{0.90}Sr_{0.10}Mn_{0.75}Fe_{0.25}O_3$/CS10MF25O (promising composition from WP2 studies but not thoroughly evaluated until submission of this deliverable).

In addition to the choice of the specific powders, it is of prime importance to have a solid general plan/approach to pursue the target of scaled-up redox structures manufacturing. This was *a priori* defined from work in WP2 and WP3 and its evolution for the case of CS10MO is provided in Figure 1 below. Initially, the plan was to proceed with the redox powder synthesis, milling of the synthesized powder, shaping and calcination of structured bodies (route #1). This route and results in terms of lab-scale specimens and studies have already been analysed in detail in WP2 and WP3 submitted deliverables. As relevant studies were progressing and with feedback from WP6 which indicated that the straightforward route#1 is quite energy intensive, a decision to test a simplified approach, as outlined in route#2 of Figure 1 was made. Preliminary positive results from the feasibility of this approach and associated energy/carbon footprint savings were analysed and estimated in D3.3 (and thus will not be repeated here). In the present deliverable, emphasis is also put in demonstrating that **route#2 can be also feasible/effective for the preparation of the scaled-up structures required for the assembly of the WP5 unit**. This is done by direct comparison of the two routes using lab-scale honeycombs and emphasizing on key-properties of interest in terms of ABCSPF's concept.

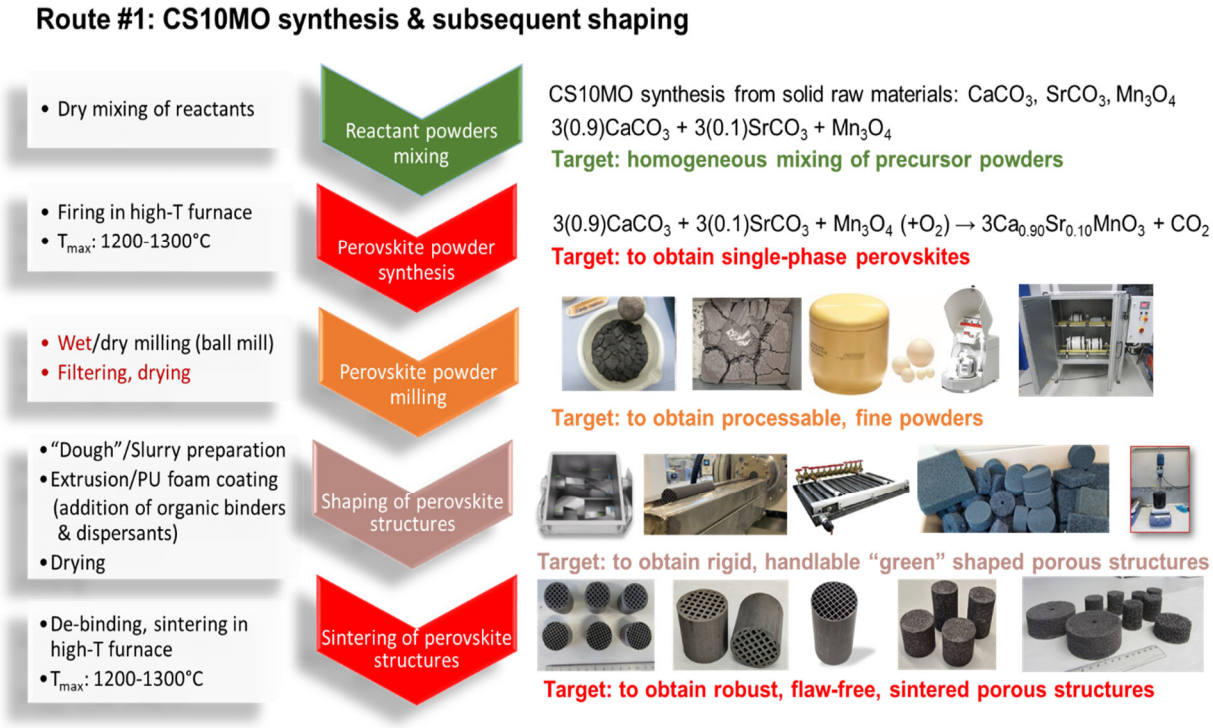

a)

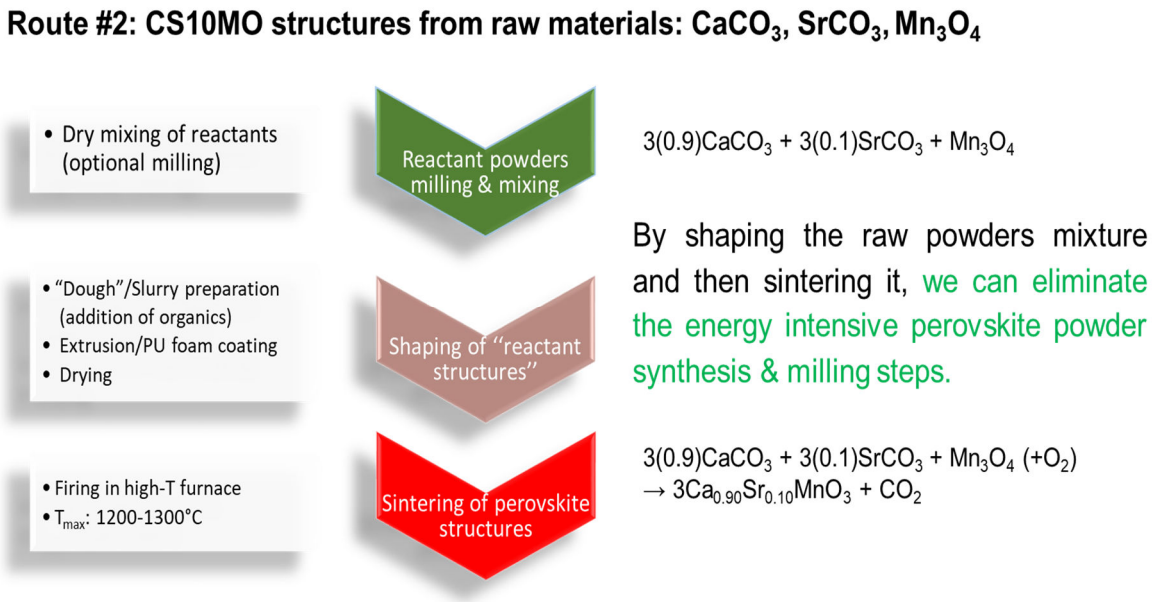

b)

Figure 1: The two routes for the preparation of perovskite structured bodies: a) the straightforward/conventional one involving the full powder synthesis-milling-shaping-sintering path; b) the simplified/energy-saving approach involving the shaping of structures from (fine) raw powders and perovskite synthesis/structure sintering steps merged into one.

Firing/calcination temperatures of structures in Figure 1 are mentioned as 1200-1300°C because in WP3 and in particular for route #1 it has been confirmed that even 1200°C is sufficient to obtain stable and quite robust structures. However, at 1300°C improvement in mechanical properties is considerable and this higher temperature is

preferable. This aspect is also briefly analysed for route #2 later in the text. It must also be mentioned that although the present deliverable refers to ''optimized redox powders'' in its title, all assessments are made on the basis of the corresponding model structured specimens from such powders because, irrespectively of the route chosen, the synthesis method relies on solid state reactions among the same powder precursors and thus any parametric analysis referring to ''powder synthesis'' per se, other than that already presented in WP2 deliverables, would have no value. All valuable information should be sought to the feasibility and effectiveness of preparing scaled-up redox structures via a tangible and as least as possible energy-intensive path.

3. Scaled-up powder synthesis

Solid-state powder synthesis routes were selected for production of scaled-up quantities of CS10MO perovskite powder, due to their scalability and the commercial availability of inexpensive raw materials (see Figure 1) in large quantities. As described in the 1st Periodic Report, various sintering temperatures in the range 1200-1350°C were tested, wherein formation of single-phase perovskite materials is favored. However, the higher the sintering temperature and the longer the dwell time therein, the more intense sintering becomes. Therefore, parametric studies with respect to phase composition (XRD) were carried out to optimize the dwell temperature in order to achieve single-phase perovskite of a phase purity as high as possible, mitigating simultaneously the adverse sintering effects. Figure 2 shows the phase composition of the products as a function of the dwell time at the sintering plateau temperature of 1200°C; given the error margin of the quantitative XRD analysis, the phase purities of the five products can be considered practically equal, indicating that **at a sintering temperature of 1200°C, a sintering time of 2 hours suffices to result in almost single-phase perovskite product;** further increase of the dwell time has no practical effect. Nevertheless, it has to be mentioned that this analysis was performed in lab-scale powder quantities of the order of few tens of grams; it is reasonable to expect that somehow higher minimum dwell times during sintering of powder quantities scaled-up to the levels of several tens of kilograms would be required to achieve similar phase purity, or, alternatively, that the phase purity of the resulting powder will be slightly lower should the dwell time be the same.

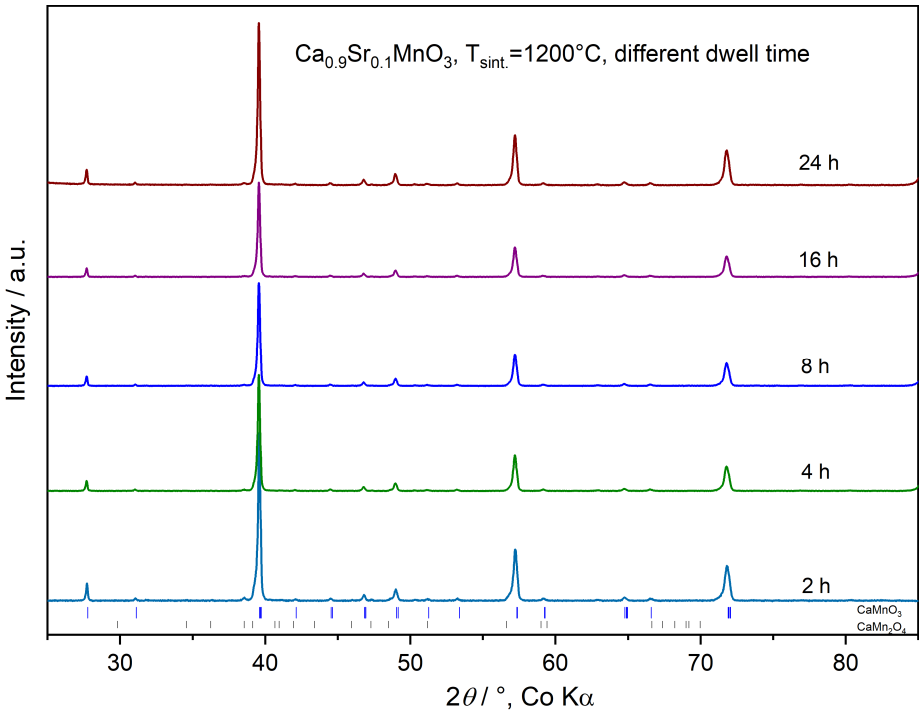

(a)

(b)

Phase fractions, wt.%	Dwell time, h				
	2	4	8	16	24
$CaMnO_3$	98.0	97.3	96.3	97.0	96.9
$CaMn_2O_4$	2.0	2.7	3.7	3.0	3.1

Figure 2: Phase purity of CS10MO perovskite powder as a function of dwell time at sintering plateau temperature of 1200°C: (a) XRD spectra of respective powders; (b) quantitative phase anylysis results: the major phase is the desired perovskite phase $CaMnO_3$ (incorporating 10 at% Sr dopant) and minute quantities of the only secondary phase, marokite, $CaMn_2O_4$ are present.

However, as already mentioned the mixtures of the perovskite precursor powders are prone to substantial sintering upon calcination at temperatures > 1100°C which are required for the formation of the mixed perovskite phase (Figure 2a). Therefore, intensive milling of the sintered powder is required in order to reduce its particle size and distribution to the fine levels required for the preparation of either pastes with rheology for extrusion or stable powder slurries for preparation of foams – usually substantially below 10 μm. At first such powders were dry-milled in a planetary ball mill (Figure 3b); it was found that dry milling with zirconia grinding media for 30min with a rotational speed of 450rpm could achieve a desired particle size distribution (PSD) with a mean particle diameter of 6.5 μm. However, the capacity of such an intensive-milling device is limited to 250 g of powder per batch; therefore, a roller jar mill device (Figure 3c), capable of milling much higher quantities of powder, ~ 10-15 kg, per experiment was purchased and employed for milling efficiently and within a reasonable time high quantities of powder. Again, by experimenting and optimizing the processing conditions, **powder quantities of the order of 10 kg can be dry-milled to the desired particle size in three hours** (Figure 3d). Such powders can then be equally well used for both processing routes, extrusion and slurry-coating for the preparation of honeycombs/foams respectively as described in detail in several WP3 deliverables.

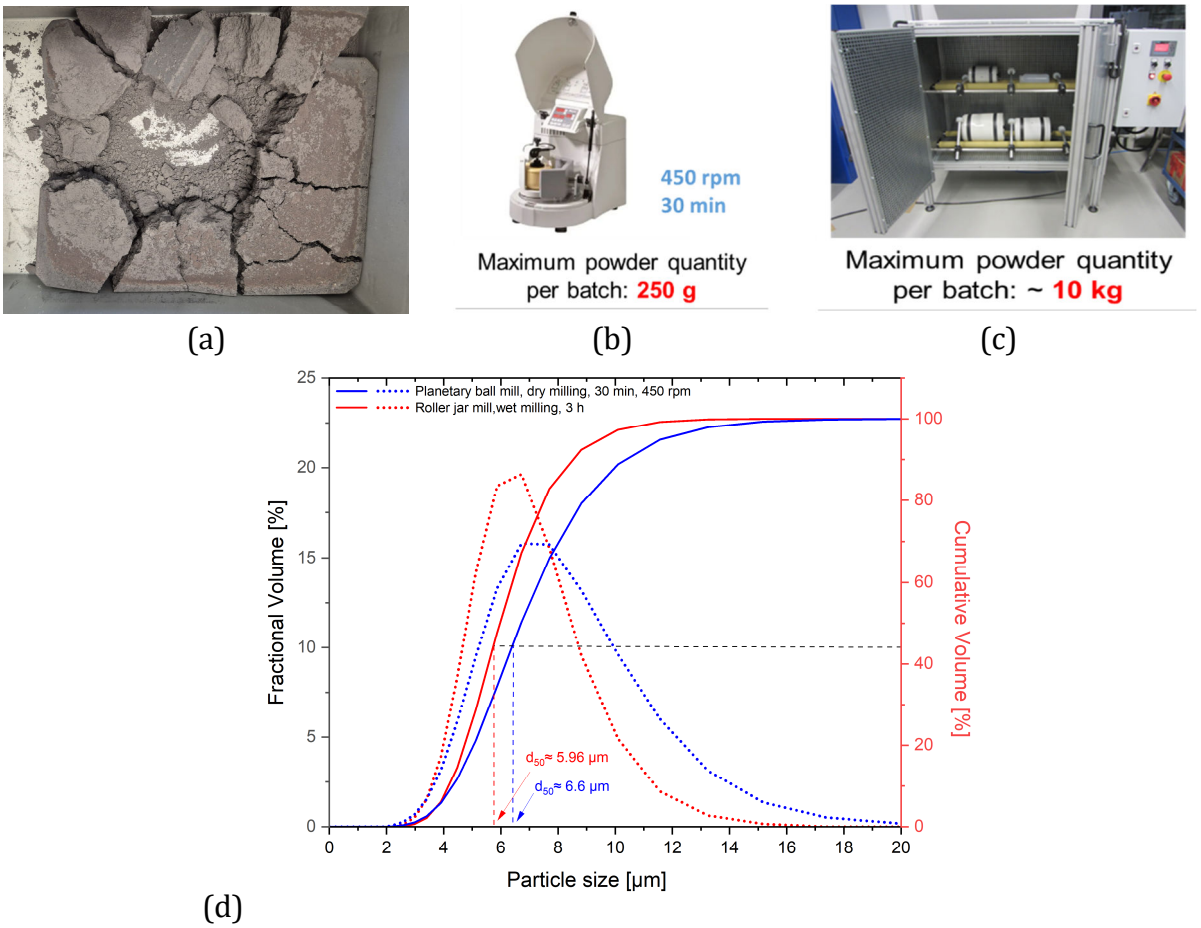

Figure 3: (a) Heavily sintered perovskite powder (batch of 1.5 kg sintered in a square crucible, single-piece product already broken down to smaller pieces with a mortar); (b) planetary and (c) roller jar mill employed for particle size reduction; (d) comparative particle size distribution achieved for the perovskite powder to be used for further processing.

4. Scaled-up powder processing

4.1 Comparison between lab-scale structures prepared via route #1 and route #2

The important attributes that are comparatively evaluated for the two different routes and in order to assess the feasibility of route #2 are listed below and further analyzed later in the text. In all cases, structures prepared by route #2 are compared to the ones prepared via the standard approach (route#1) in terms of their:

- **Chemistry and redox performance**: it is important to verify that the structures prepared via the two routes have the same or at least comparable a) purity in terms of the targeted redox-active phase (i.e. CS10MO) and b) redox performance in terms of both reduction extent (defined by the non-stoichiometry factor δ) achieved and stability in the course of multi-cyclic redox operation (up to 1100°C).
- **Mechanical and geometric characteristics**: similarly, the comparative geometric characteristics and most importantly the sufficient mechanical stability

- **Behaviour of scaled-up redox specimens prepared by route #2 during their calcination/sintering**: should the attributes mentioned above are assessed as satisfactory for the case of route #2, it is also very important to ensure that the scaled-up structures can be calcined/sintered to obtain robust and free of any major defects redox bodies.

4.1.1 Purity in terms of the targeted redox-active phase

As elaborated in several deliverables, two kinds of structures have been manufactured so far in the project, namely honeycombs and reticulated porous ceramics (RPCs) – the latter commonly known as ceramic foams. However, foams have been so far manufactured only via route #1, i.e. from pre-synthesized perovskite powder. XRD spectra of powders from such crashed and finely ground porous structures made via both routes and sintered at the same temperature of 1300°C, are shown in Figure 4. It is evident that not only the products from every route are single-phase perovskites (all peaks correspond to this structure) but also products from the two routes (in the case of extruded honeycombs) are practically identical.

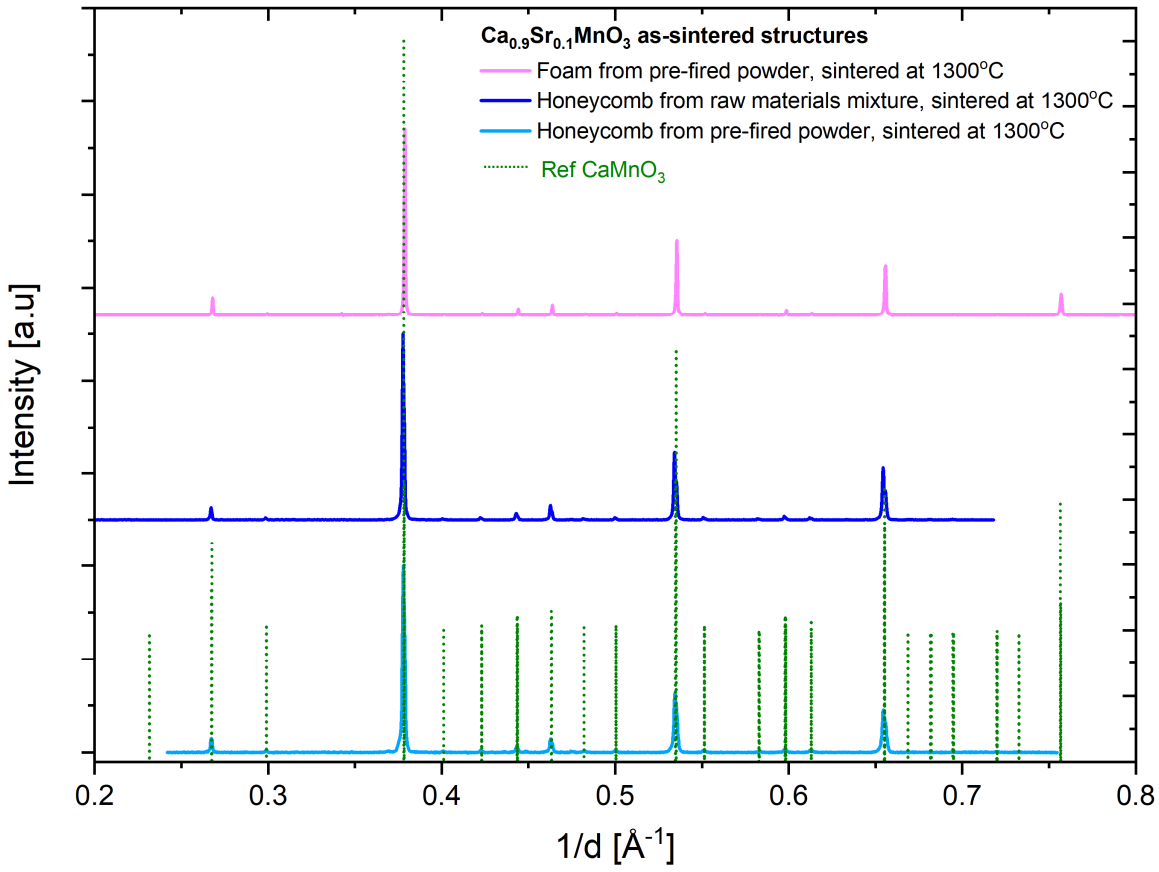

Figure 4: XRD spectra of CS10MO representative porous structures manufactured through both routes.

4.1.2 Mechanical robustness

The porosity of a structure largely defines its robustness and (thermo-)mechanical stability. Thus, Figure 5 provides comparative porosimetry measurements for small-scale honeycomb structures prepared by CERTH with the same extrusion die (i.e. 44 cpsi) but following the two different routes. It also depicts the effect of the calcination temperature of the structure to its porosity (route #2 only). Evidently and as also further analyzed and explained later in the text, the structure prepared by route #2 results to measurably higher porosity than the one from route #1 (i.e. 33.1% vs 24.6%) while its pore size distribution is clearly shifted to higher values (i.e. larger pores). The calcination temperature for a given manufacturing route (route #2) plays a much more profound role as the structure sintered at 1200^{o}C has a porosity of as high as 57.5%, compared to the aforementioned 33.1% for the honeycomb calcined at 1300^{o}C. This highlights the importance of a sufficiently high calcination temperature on obtaining sufficiently dense/robust bodies, which should not be underestimated or compromised for e.g. the sake of e.g. (limited) energy saving. The sintering temperature does not significantly affect the pore size distribution but mainly the total porosity of the honeycomb. Note that all 3 samples depicted here were prepared from the same 44 cpsi extrusion die but different preparation conditions will result to slightly different cpsi values; both the calcination temperature and the preparation route affect cell density in a profound way. Calculated bulk densities of the structures analyzed in Figure 5 are in full agreement with the findings reported therein; i.e. 2.25 g·ml^{-1} for the CS10MO – route 1 @1300^{o}C, 1.91 g·ml^{-1} for the CS10MO – route 2 @1300^{o}C and 1.45 g·ml^{-1} for the CS10MO – route 2 @1200^{o}C.

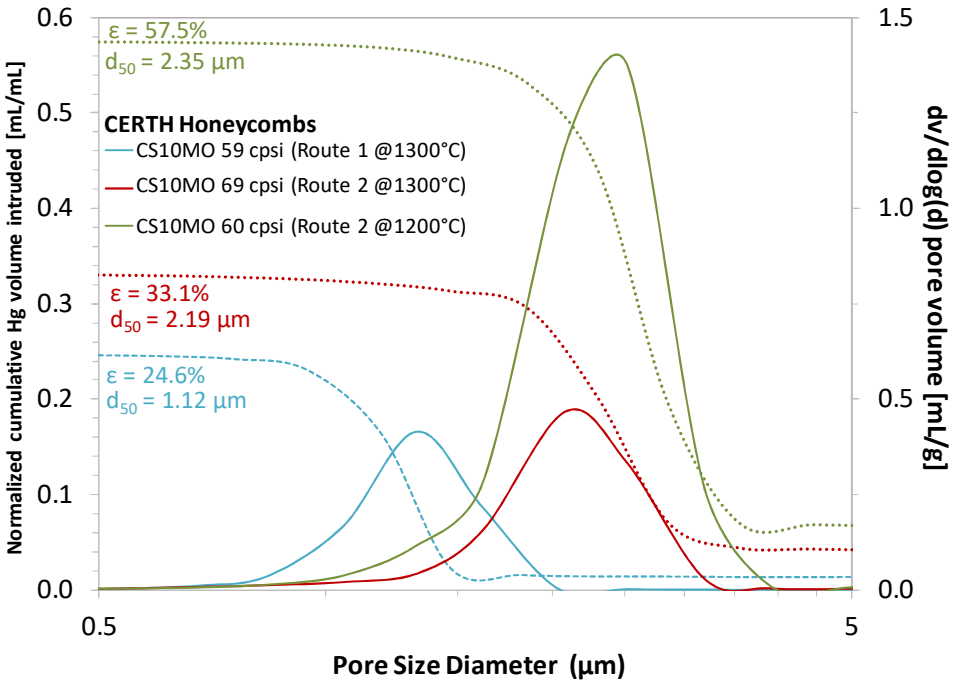

Figure 5: Comparative mercury porosimetry measurements indicating the notable differences between honeycombs prepared by routes #1 and #2 and calcined at 1300^{o}C as well as by route #2 and calcined at 1200^{o}C or 1300^{o}C.

Compressive (crushing) strength tests were performed on CS10MO honeycomb specimens produced via route 2 to be compared to those on similar specimens produced via route 1 reported in D3.2. This comparison as well as further comparison to "reference" commercial, non-redox cordierite honeycomb specimens of 3 different cell densities, is shown in Figure 6. There is indeed a difference between the maximum compressive stress of the honeycomb from the pre-fired powder vs. that of the raw-materials-mixture-extruded one - 60 MPa vs. ca. 32 MPa – however this is directly correlated to the much higher porosity of the latter structure. Nevertheless, the strength of the honeycomb produced through route#2 is almost double that of commercial cordierite honeycombs.

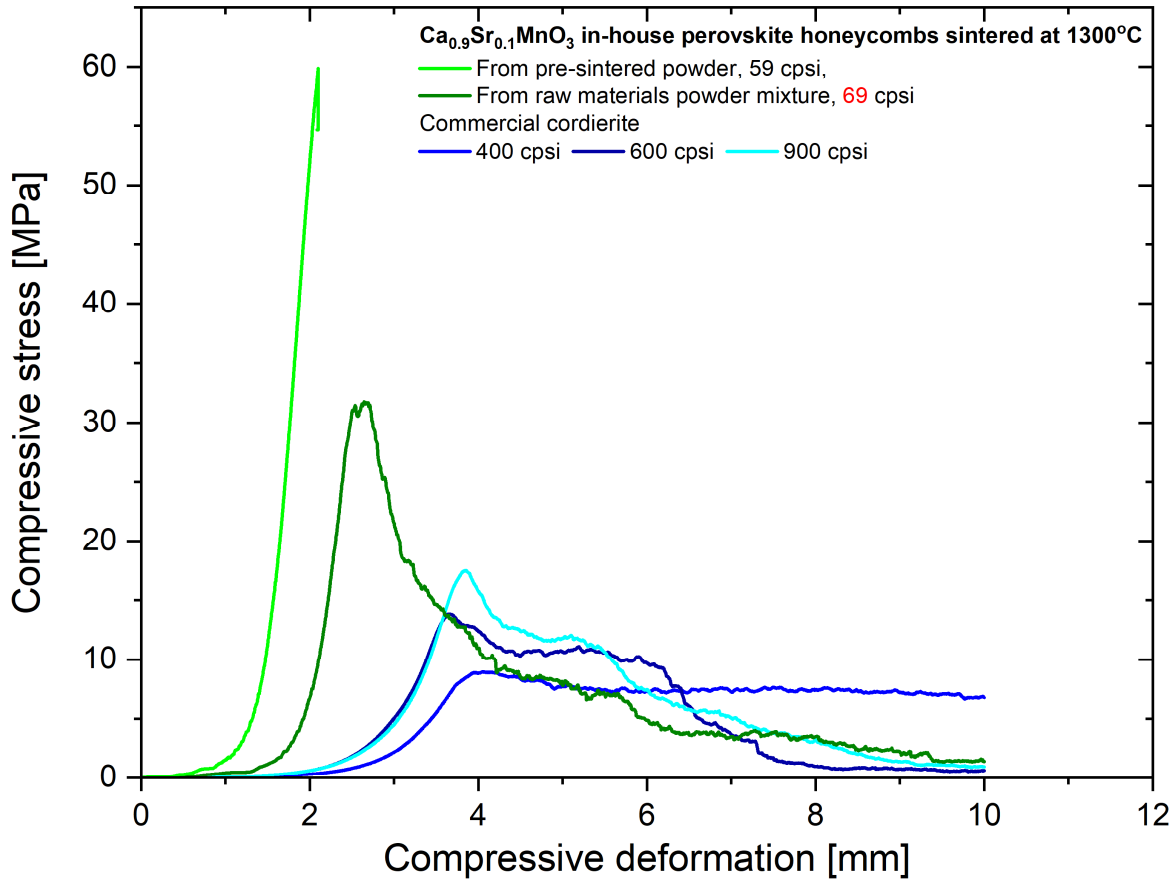

Figure 6: Compressive stress-deformation curves of in-house produced CS10MO honeycombs produced via the two routes, in comparison to commercial cordierite ones.

4.1.3 Comparative redox performance

In terms of redox performance, Figure 7 presents a direct comparison between two 59-69 cpsi honeycombs (using the same 44 cpsi die/see deliverables D3.1 and D3.3 for relevant photos) prepared by the two different routes described above. Moreover, Figure 8 shows the value of non-stoichiometry factor (δ) with the number of redox cycles carried out per case. As already explained in the submitted deliverables of WP2, δ provides a direct measure of the reaction extent as it corresponds to the amount (in mol) of O_2 released/consumed during the reversible redox reaction per 2 mol of the perovskite. The

main redox parameters are summarized in Table 1. Evidently, redox performance is not affected by the route followed to prepare the perovskite structured body. The two honeycombs behave identically and show excellent cycle-to-cycle repeatability.

a)

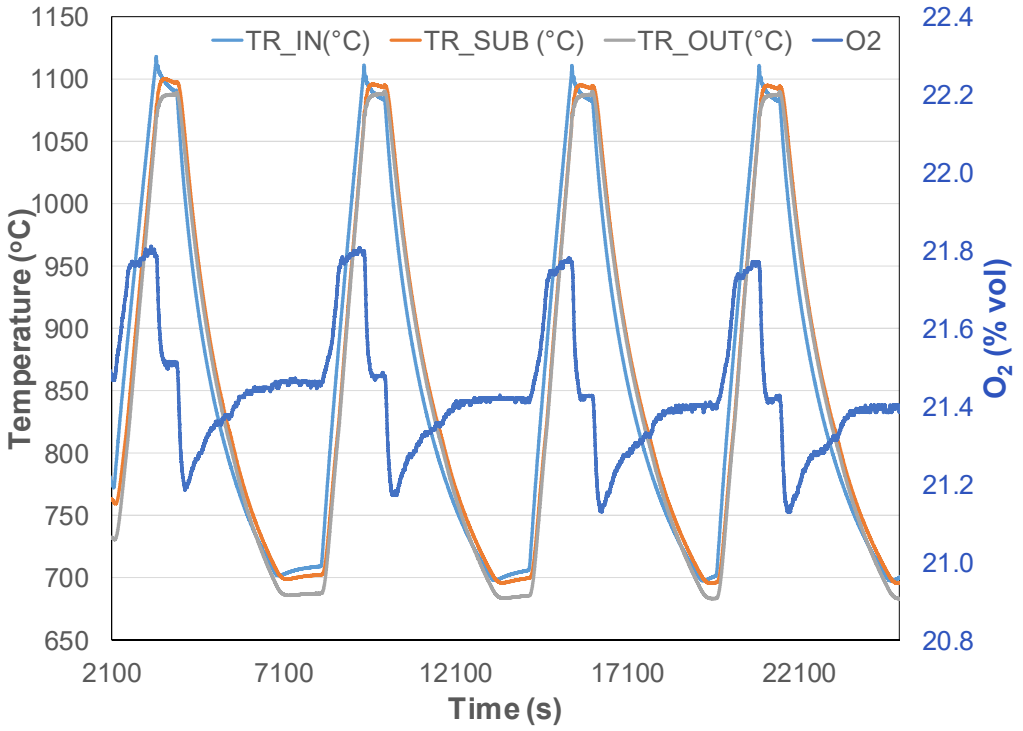

b)

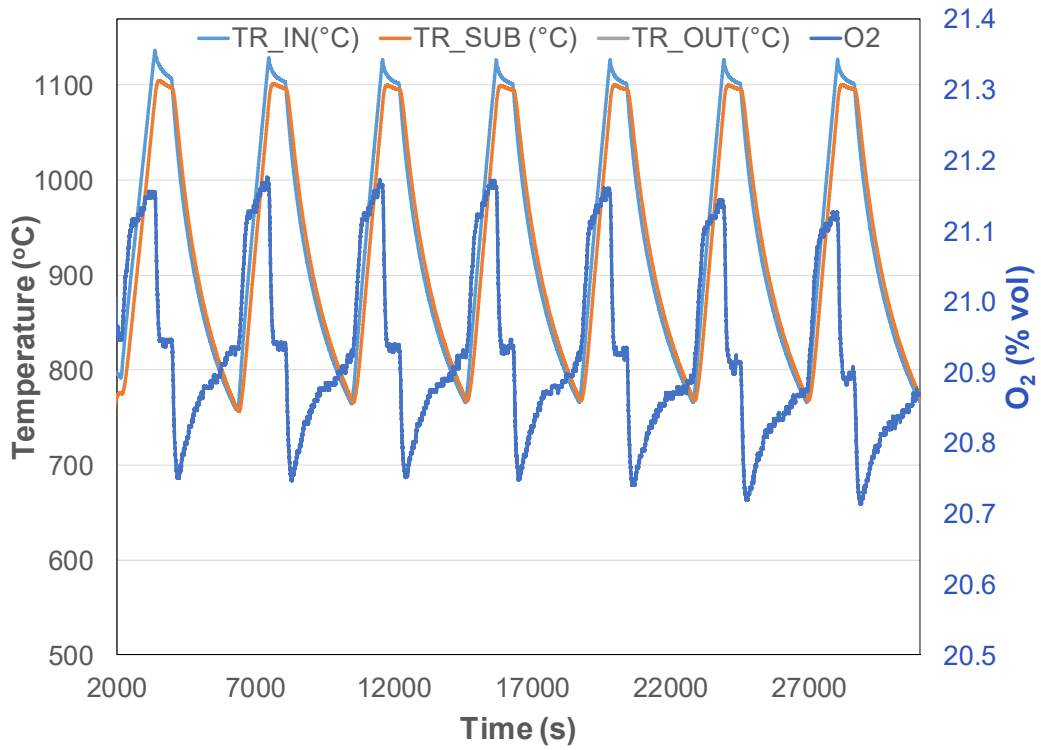

Figure 7: Indicative redox cycles showing the O_2 release/consumption during heating-up/cooling down of specimens in air flow: a) 4 cycles from the CS10MO honeycomb prepared via route #1; b) 7 cycles from the CS10MO honeycomb prepared via route #2. All experiments were carried out with the aid of the test-rig presented in deliverable D3.2

a)

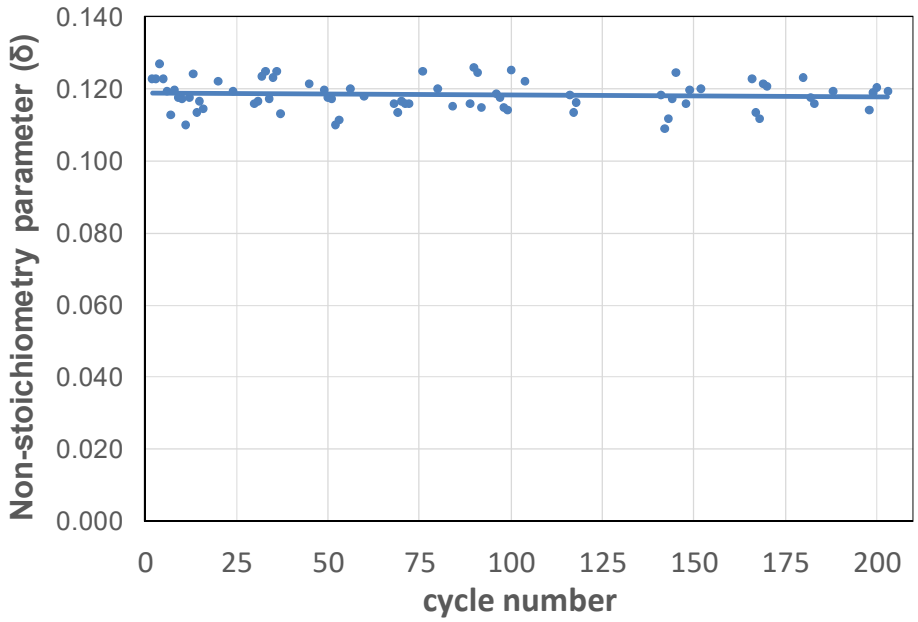

b)

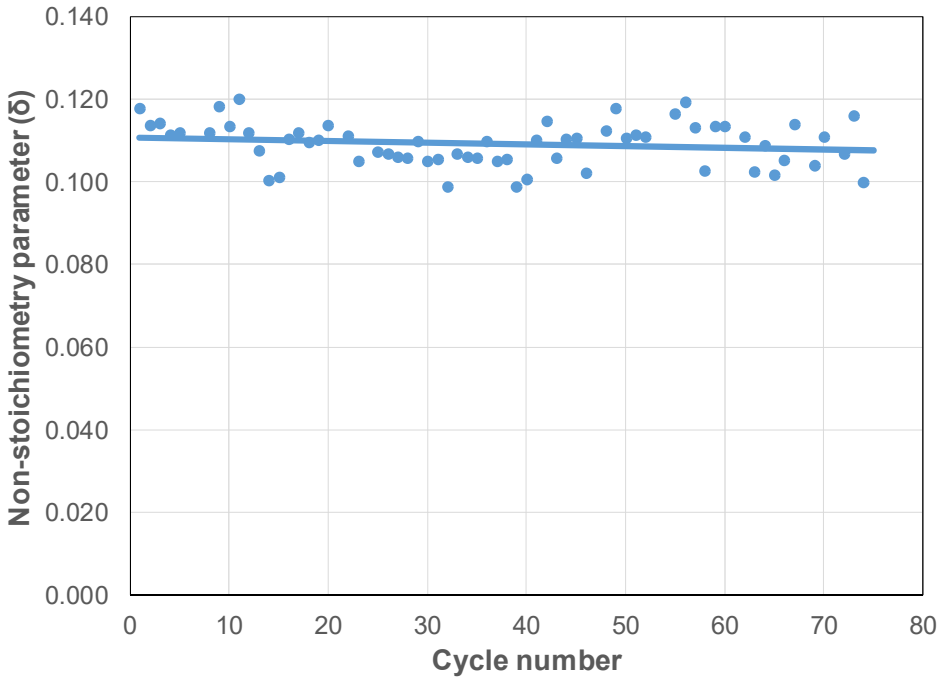

Figure 8: Variation of δ with the number of redox cycles as derived from multiple experiments in accordance to Figure 7: a) CS10MO honeycomb prepared via route #1 (203 cycles in total); b) CS10MO honeycomb prepared via route #2 (75 cycles in total). Points refer to real experimental measurements & the lines are added to highlight the stability of cycle-to-cycle performance

Structure	O_2 in reduction (mmol/g)	O_2 in oxidation (mmol/g)	δ (average)
59 cpsi CS10MO honeycomb - route#1	410 ± 15	399 ± 14	0.118 ± 0.004
69 cpsi CS10MO honeycomb – route#2	382 ± 24	392 ± 43	0.113 ± 0.007

Table 1: Main redox parameters for the two extruded CS10MO honeycombs prepared by different routes as derived from the respective multi-cyclic experimental campaigns.

4.2 The structures' scaling-up challenges and proposed solution(s)/risk mitigation measures

As already implied in the submitted deliverable D3.3 and is also well-known to LET, the size of the cross-section of extruded green honeycombs relates directly with the easiness or even feasibility of obtaining dried and, most importantly, sintered structures that will be free of any major defects and sufficiently robust to be handled and used inside a thermochemical reactor. Naturally, the higher the size of the cross section and of the overall segment to be dried/sintered, the more difficult it becomes to obtain stable and robust finished honeycombs. Other very or even equally important parameters to be considered and known or expected to affect the manufacturing process are:

- The nature and behaviour of the material(s) comprising the as-received extruded structure.
- The geometry of extruded channels; i.e. for a similar cell density and overall shape, structures with round channels are normally more stable and robust than the ones with tetragonal channels.
- The thickness of the honeycomb walls and the cell density of the structure. Thicker walls and structures of lower cell density are easier to extrude cf. more delicate structures with more cells per unit area of the cross section.

Selected parameters among the above are analysed separately based on relevant experimental results obtained so far and relevant risk mitigation measures are identified. At the time of preparation of this deliverable additional to the ones analysed here parametric studies to cover all the above were in progress.

4.2.1 Size of extruded cross-section

The increase in the targeted size of cross-section of structured bodies induces challenges even from the paste extrusion and subsequent drying steps. To visualize this, Figure 9 shows two similar – extruded by LET – cylindrical geometries with square channels and diameter values of 80 mm and 118 mm, both produced from identical pastes of raw mixtures (i.e. route #2) corresponding to the CS10MO stoichiometry. Evidently, the higher diameter resulted to cracked green honeycombs. It is noted that some cracked structures were also produced for the case of the 80 mm diameter but, contrary to the 118 mm ones, the vast majority of manufactured such segments were crack-free. Naturally, the larger cpsi (channel density) value of the 118 mm geometry has also played its role but this particular parameter is further analysed in paragraph 2.2.3.

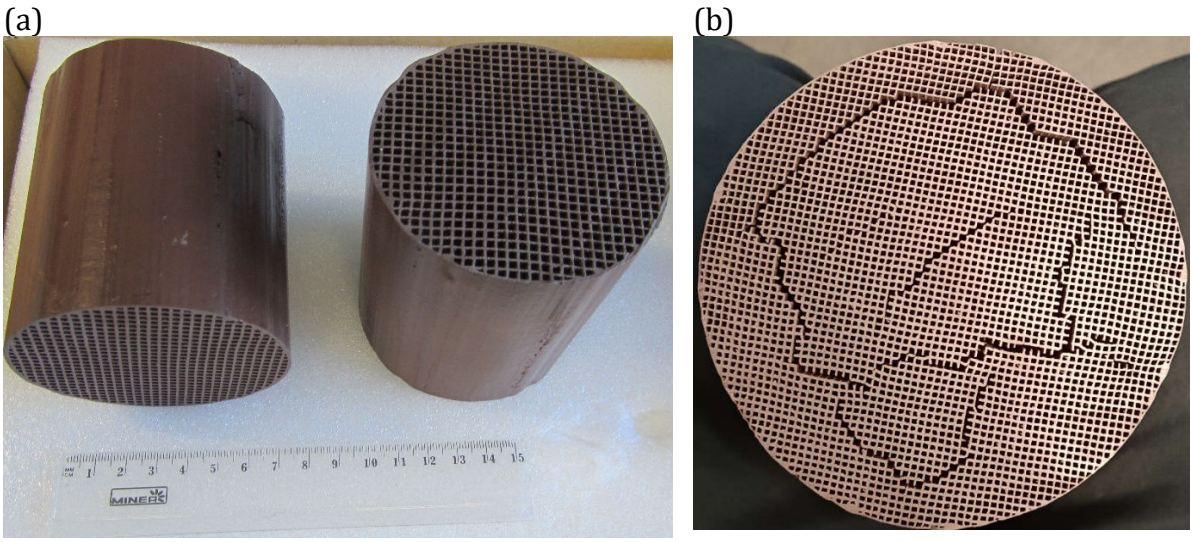

Figure 9: Extruded dried honeycombs by LET: a) 80 mm diameter using a 90 cpsi extrusion die (macroscopically defect-free samples); b) 118 mm diameter using a 200 cpsi extrusion die (cracked sample). The negative effect of increasing the cross-section size is evident.

4.2.2 Nature and behaviour of materials extruded

This aspect has already been analysed in deliverable D3.3 to a certain extent and relates to the generation of profound amounts of gases in the process of calcining the green bodies to obtain the required final sintered bodies. Based on an overall assessment at LET during the parametric studies of scaled-up extrusion, it was concluded that the macroscopic behaviour and overall rheological characteristics of extrudable pastes prepared from the CS10MO-based raw materials mixture is similar to SiC-based pastes routinely prepared and extruded by LET for commercial purposes. This was an initial positive finding because it provided confidence on the in-principle feasibility of the relevant activities and plan.

The use of organic materials such as binders and/or agents to ensure that the pastes to be used have proper rheological characteristics and coherence to yield as-received honeycombs of sufficient quality is a standard approach in extrusion. During de-binding and firing of the structures, these organic materials are removed via combustion and thus the corresponding amounts of CO_2 and H_2O evolve from the bulk mass. This happens at temperatures of about 200-500^{o}C and naturally up to that point the structures become quite porous and their coherence is minimal. As mentioned, the use of carbonates as precursors for the corresponding oxides to be formed which will later react to form the CS10MO perovskite phase results to an additional substantial amount of CO_2 gas evolution from the bulk structure. This decomposition of carbonate-precursors occurs in the range of 550-890^{o}C and further magnifies the aforementioned loss of structural coherence issue initially caused by the organics' removal. To obtain an overview of the quantitative mass loss profile and associated temperature ranges, a representative Thermo-Gravimetric Analysis (TGA) profile as obtained for a small fragment from a dried scaled-up structure

extruded at LET is provided in Figure 10. The above-mentioned weight losses are clearly detectable in the TGA profile and are indeed substantial. The low temperature (i.e. < 200°C) small mass change is attributed to residual humidity removal while the second and substantial more intense loss (~200-360°C) is due to removal (evaporation, combustion) of organic additives in the extrusion paste (e.g. binder etc.). Up to that point the cumulative weight loss is already about 9-10%. In the window of approximately 550-890°C, the main mass loss occurs and corresponds to the dissociation of carbonate salts precursors. The first profound decrease is due to $CaCO_3$ decomposition and the last higher-temperature one is due to $SrCO_3$. The slight weight increase just above 900°C (see mass change curve) correlates to the onset of the solid state reaction among the formed single oxides (i.e. CaO + Mn_3O_4/Mn_2O_3 and SrO), which also requires uptake of O_2 from the imposed air flow.

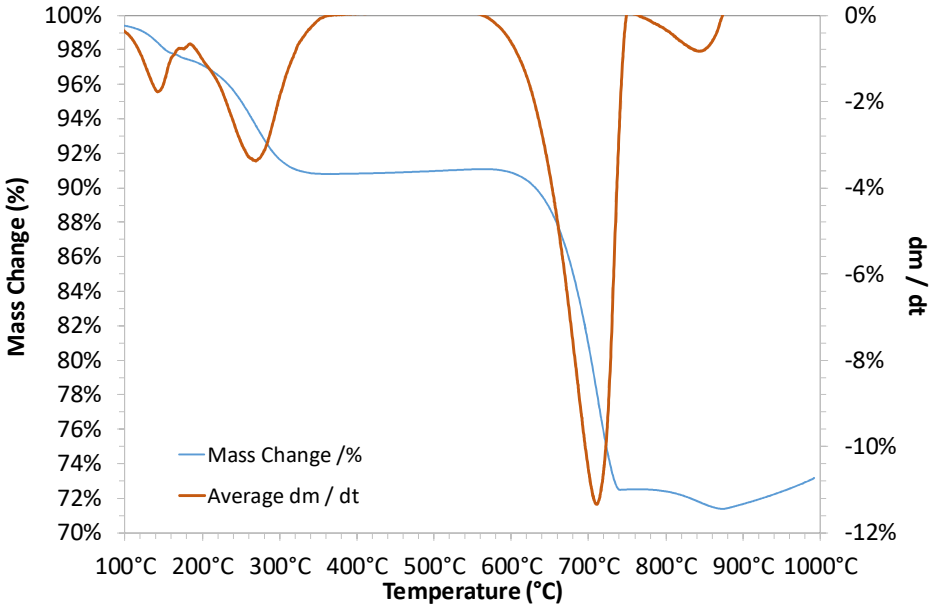

Figure 10: TGA profile and its derivative curve as obtained for a green scaled-up structure extruded at LET. The analysis was done under air flow.

Naturally, by about 900°C the structure has become extremely loose due to the cumulative removal of gases from its bulk mass. Further heating, results to its gradual sintering and, as mentioned earlier, above 900°C the solid state reaction among the 3 oxides (CaO, Mn_3O_4, SrO) starts to take place gradually thereby also facilitating the sintering process. Due to the profound porosity generated by cumulative gases evolution, the structure leaves substantial potential for shrinkages until the maximum firing temperature of 1300°C is reached. To macroscopically quantify the shrinkages and other important characteristics of sintered vs green honeycombs that provide the challenges associated to the nature and behavior of project's materials extruded, these are summarized in Table 2 and to some extent visualized in Figure 11.

The measured loss is in general agreement with the overall weight loss identified by the TGA analysis mentioned above while shrinkages are notable (~20%). To put the latter

in perspective, the respective typical shrinkages for commercial fired SiC structures extruded by LET are as low as 3-4%. Evidently, the difference is profound and according to LET's expert opinion shrinkages on the order of 20% directly challenge the limits of feasibility of structures' structural integrity during sintering, thereby indicating the importance and necessity of precise process control.

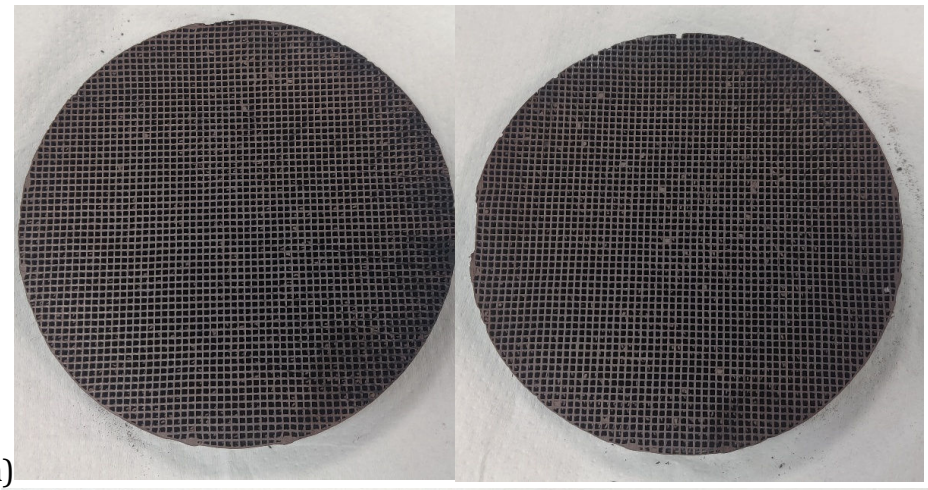

(a)

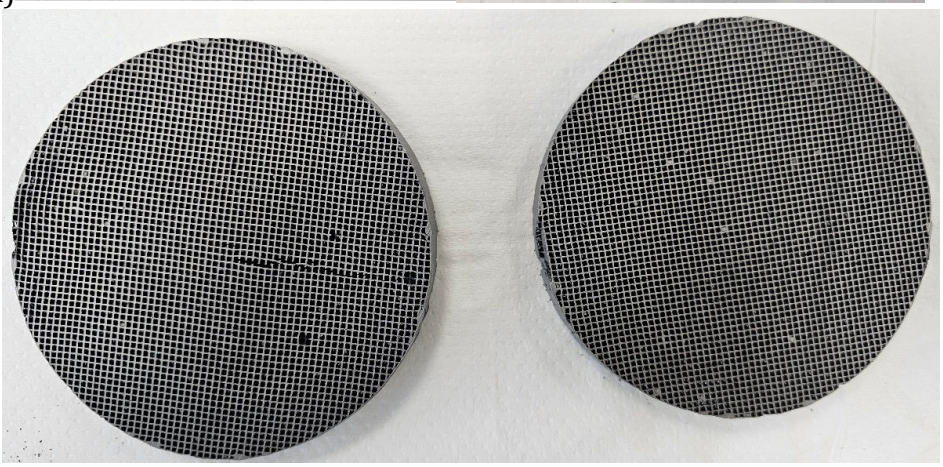

(b)

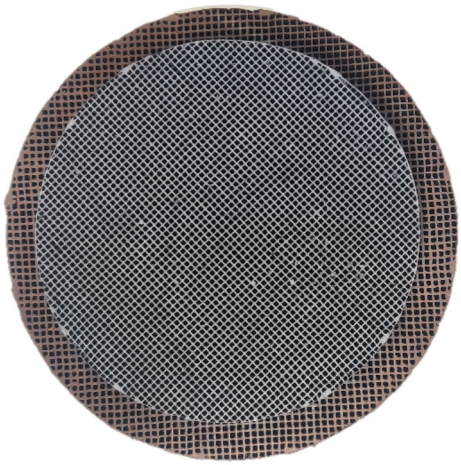

(c)

Figure 11: Photographs of two 15 mm in height segments sliced from ∅ 118 mm green honeycombs before (a) and after (b) their calcination at 1300°C. Green sliced honeycombs in (a) were selected among several sectioned to be macroscopically defect-free. In (c) the calcined segment is placed on top of an identical green one to help visualization of the profound shrinkage caused by the firing process

Dimensional changes		Mass change (%)	Bulk/geometric density of sintered structure (g·ml^{-1})	cpsi of sintered body
Diameter (%)	Height (%)	~ - 38.6	~ 1.12	323
~ - 19.8	~ - 19.8			

Table 2: Main macroscopic properties as directly measured or calculated after calcination at 1300°C of the 15 mm-thick sliced segments depicted in Figure 11.

4.2.3 Effect of cell density in combination with the cross-section size

Figure 12 shows an indicative and representative result of calcination at 1300°C of sliced (approximately 15 mm thick as the ones in Figure 11) segments sectioned from the green honeycombs of Figure 9a (∅ 80 mm, extruded with the 90 cpsi die). As can be seen, calcination was successful as both sintered bodies had only minor defects. There was no detectable deformation in either of the sintered slices and those were sufficiently robust and easily handleable. The result was equally good or even slightly better that the one presented in Figure 11 for the ∅ 118 mm slices extruded with the 200 cpsi die. This indicates that switching to a less delicate structure facilitates the process. As also revealed from the left segment of Figure 11b that clearly showed limited defects after calcination despite being visually flawless in its green state, a higher cell density/high diameter body is more prone to propagation of, even undetectable by the naked eye, flaws caused by extrusion and/or drying as compared to the thicker geometry of Figure 12.

Table 3 provides an overview of the main macroscopic changes due to calcination as well as the bulk density and measured weight loss referring to the segments of Figure 12. As expected, the results are very similar to the ones shown in Table 2 for the more delicate/of-larger-cross section structure.

Table 3: Main macroscopic properties as directly measured or calculated after calcination at 1300°C of the 15 mm-thick sliced segments depicted in Figure 12.

Dimensional changes		Mass change (%)	Bulk/geometric density of sintered structure (g·ml^{-1})	cpsi of sintered body
Diameter (%)	Height (%)	~ -39.0	~ 1.26	139
~ -20.4	~ - 21.3			

Table 4: Main macroscopic properties as directly measured or calculated after calcination at 1300°C of the 15 mm-thick sliced segments depicted in Figure 12.

(a)

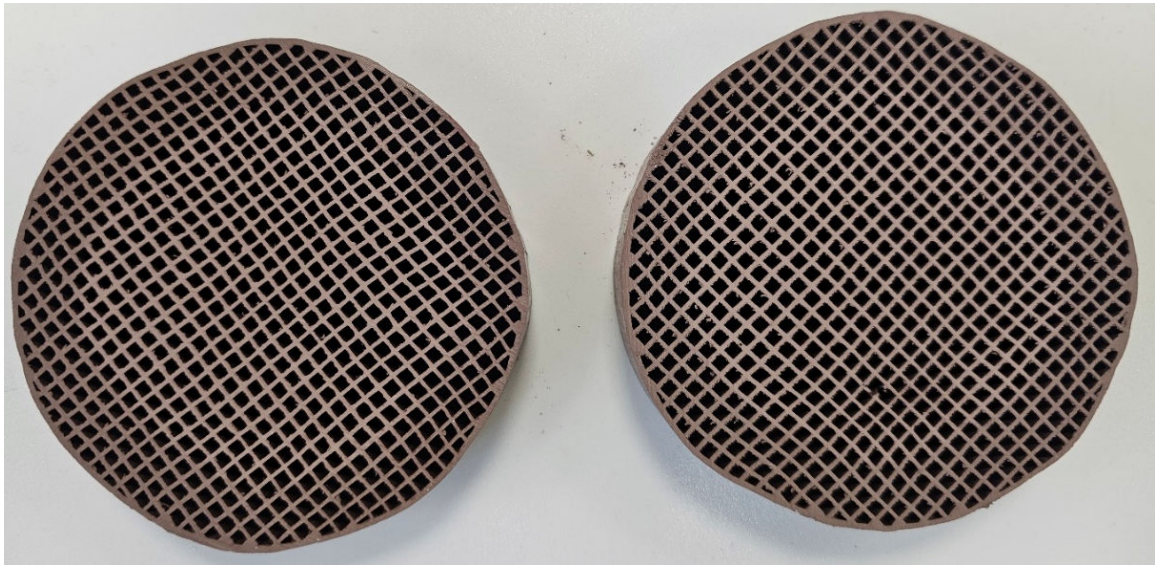

(b)

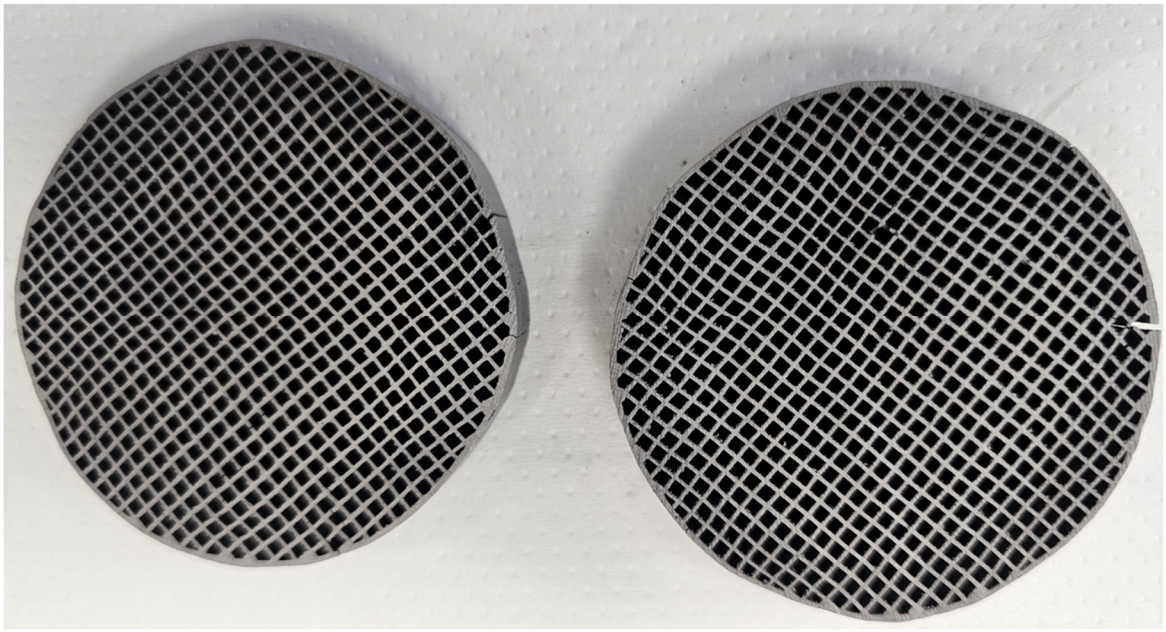

Figure 12: Representative comparative photographs of: a) sliced (approx. 15 mm thick) green bodies from the honeycombs in Figure 9a and b) the ones in a) after their calcination at 1300°C

Additional attempts to mitigate the (mostly minor) defects and further improve the quality of calcined honeycombs, while increasing the thickness of the segments to well above 15 mm are currently underway. At present the main parametric study to achieve this relates to further modification and fine tuning of the calcination protocol; namely introduction of additional slow heating and isothermal steps at identified crucial temperature ranges.

5. Main conclusions and plan for achieving the final scaled-up structures to assemble the proof-of-concept dual bed unit

Currently the **most favorable geometry relates to cylindrical honeycombs** but those **need to be sliced to segments** of about 15 mm in thickness to minimize the number of cracks in the final calcined body. Considering that for the ∅ 118 mm/200 cpsi (nominal/raw segments) geometry, extrusion and drying are quite challenging and the success rate of obtaining such in green form is already very low, **the most feasible option seems to be the ∅ 80 mm/90 cpsi** (nominal/raw segments) option.

As of submission of the present deliverable, **route#2 as depicted in Figure 1 and analyzed here is the qualified plan to follow**. However, the challenges need to be resolved/mitigated and the consortium is still working towards this direction with some considerable progress already achieved and reported here. Further improvements and validation of reduction of consistent results would provide more confidence on the choice made here. Important guidelines to be considered are summarized as:

- Choice of a relatively **low cpsi/thick walls geometry** helps obtaining more stable structures and this applies to the whole process chain; i.e. from extrusion, to drying to calcination/sintering.
- One needs to consider that minimization/elimination of defects (cracks, deformation) is most likely achievable by **slicing the honeycombs in relatively thin** (e.g. 15 mm) **segments** and calcining them based on the customized protocol extracted from the TGA analysis of green bodies.
- **Calcination/sintering needs to be very slow and carefully executed**. Further customization/optimization compared to the protocols applied here (i.e. largely based on findings extracted from the analysis in Figure 10) may be necessary and other factors such as the architecture of the furnace used for such sintering may also be important and a relevant study (not carried out yet) would be also advisable.
- **The profound gases evolution referring to route#2 may mean that certain compromises are necessary**, at least at such early developmental stage; i.e. sintered bodies will not necessarily need to be perfect but in a useable form. This is likely to affect negatively the thermo-mechanical robustness of the structures upon multi-cyclic operation but the task is very challenging and may in fact be a separate project by itself.